



Characterization and photocatalytic activity of TiO₂ nanoparticles on cotton fabrics, for antibacterial masks

Marco Antonio Alvarez-Amparán¹ · Vanessa Martínez-Cornejo¹ · Luis Cedeño-Caero¹ · Kevin A. Hernandez-Hernandez^{2,3} · Rubén D. Cadena-Nava² · Gabriel Alonso-Núñez² · Sergio Fuentes Moyado²

Received: 28 June 2022 / Accepted: 30 August 2022
© King Abdulaziz City for Science and Technology 2022

Abstract

The *in-situ* impregnation of two commercial cotton fabrics (lab coat and Indiolino) with TiO₂ nanoparticles (TiO₂-NPs) was carried out. For this, two commercial cotton fabrics were dipped in titanium isopropoxide, titanium butoxide and titanium tetrachloride solutions to the TiO₂-NPs formation and *in-situ* TiO₂-NPs impregnation on the cotton fabric surface by the sonochemical, hydrothermal and solvothermal methods, respectively. The impregnated fabrics were characterized by ATR-FTIR, SEM-EDS, Raman, UV-Vis, DRS and tension tests. The results showed the successful formation and impregnation of TiO₂-NPs on both cotton fabrics. The leaching of TiO₂-NPs from cotton fabrics was negligible after several washing cycles. The self-cleaning properties and antibacterial activity of TiO₂-NPs functionalized cotton fabrics were assessed by photocatalytic and antibacterial tests. The photocatalytic activity was determined by the degradation of methylene blue dye under UV and solar irradiation. The materials showed good photoactivity, since MB was degraded up to 99% under solar and UV irradiations in 60 min. The bactericidal capacity of the TiO₂-NPs on fabrics, evaluated *in-situ* by SEM, showed that Indiolino presented the best antibacterial properties against *Escherichia coli* and *Bacillus pumilus*.

Keywords Titania nanoparticles · Antibacterial masks · Cotton fabrics · Sonochemical synthesis · Hydrothermal synthesis

Introduction

The development of fabrics with antibacterial and antiviral activity and self-cleaning properties has been triggered in the last decades due to healthcare industry and home textiles applications (Hussain 2020; Yocupicio-Gaxiola et al. 2021; Konda et al. 2020; Botequim et al. 2012; Montazer and Seifollahzadeh 2011). Moreover, the current COVID-19

pandemic caused by the SARS-CoV-2 virus has potentiated the exhaustive research on this type of functionalized fabrics since these ones could help avoiding the virus dispersion (Yocupicio-Gaxiola et al. 2021; Militky et al. 2021). The cotton fabrics are the main textile used in the healthcare industry since the cotton surface could be electrostatically charged, in an analogous way as on the natural silk surface (Konda et al. 2020). In this sense, since the cotton fabric is a porous and hydrophilic material, antibacterial agents can be added over the cotton surface. Also, the addition of an antiviral agent to the textile fibers is an interesting option as additional protection to avoid virus infections for both the wearer and those around them.

The selection of an antiviral agent should be based on its antiviral activity, level of toxicity, method of application and cost. Also, antiviral agents added to textile fibers must be active even in the presence of a wide class of microorganisms, stable, durable, safer for the user and not harmful to the environment. It has been shown that inorganic nanoparticles (NPs) can inactivate virus due to the viral envelope rupture by the generation of oxidant species

✉ Marco Antonio Alvarez-Amparán
malvarez@quimica.unam.mx

✉ Luis Cedeño-Caero
caero@unam.mx

¹ UNICAT, Departamento de Ingeniería Química, Facultad de Química, Universidad Nacional Autónoma de México, 04510 Ciudad de Mexico, México

² Centro de Nanociencias y Nanotecnología (CNYN-UNAM), Universidad Nacional Autónoma de México, 22800 Ensenada, Baja California, México

³ Centro de Investigación Científica y de Educación Superior de Ensenada (CICESE), Ensenada, Baja California, México

(Botequim et al. 2012; Ogunsona et al. 2020, Yaqoob et al. 2020). Also, it is important to mention that inorganic NPs may act as adsorbents, catalysts or photocatalysts, which could enhance or promote high antibacterial activity. Currently, inorganic NPs and their composites are a viable alternative to manufacture multifunctional and antiviral fibers (Hussain 2020; Yocupicio-Gaxiola et al. 2021). Among others inorganic NPs, TiO₂ nanoparticles (TiO₂-NPs) have attracted attention because they are biocompatible, non-toxic, and inexpensive (Yocupicio-Gaxiola et al. 2021). The incorporation of TiO₂-NPs on textile fibers provides them with antiviral properties, UV protection, promotes surface hydrophobicity/hydrophilicity, could act as flame retardant, and provide self-cleaning properties (Hussain 2020; Yocupicio-Gaxiola et al. 2021; Montazer and Seifollahzadeh 2011, Lessan et al. 2011; Senić et al. 2011). The antibacterial activity of TiO₂-NPs is attributed to the fact that they can produce reactive oxygen species (ROS) in the presence of UV irradiation, since TiO₂-NPs is a semiconductor material, acting as a photocatalyst. Also, TiO₂-NPs antibacterial activity has been observed in dark conditions, however, the action mechanism is not yet fully understood (Ogunsona et al. 2020).

The synthesis of TiO₂-NPs by sonochemical irradiation at low temperatures has been reported as an efficient method to obtain nanocrystals of suitable size (Guo et al. 2003). In a similar sense, Prasad et al. (2010) reported the synthesis of TiO₂-NPs by the sol–gel method assisted by ultrasound at low temperature. Additionally, the impregnation of several types of NPs on the surface of cotton fibers by ultrasonic irradiation has been reported previously, e.g., Ag nanoparticles (Hadad et al. 2007), ZnO nanoparticles (Perelshtein et al. 2009a), CuO nanoparticles (Perelshtein et al. 2009b) and TiO₂-NPs (Perelshtein et al. 2012). Akhavan et al. (2014) and Montazer and Seifollahzadeh (2011) have reported the immobilization of TiO₂-NPs on cotton using the ultrasound-assisted sol–gel method, obtaining the anatase phase without requiring subsequent heating. Complementary, cotton fabrics impregnated with TiO₂-NPs by ultrasound showed high resistance to the leaching under several washing cycles, maintaining their self-cleaning, antibacterial, and antiviral properties (Akhavan et al. 2014).

In this work, to obtain fabrics with antibacterial properties, cotton fabrics with TiO₂-NPS were synthesized by several methods. Cotton fabrics were analyzed by ATR-FTIR, Raman and SEM–EDS to assess the appropriate formation and impregnation of the TiO₂-NPs on the surface of the fibers. Photocatalytic degradation of methylene blue (MB) was carried out under UV and solar irradiation to assess the self-cleaning properties. The MB degradation rate was discussed in terms of the pseudo-first order kinetic constants. *Escherichia coli* and *Bacillus pumilus* bacteria were incubated on the functionalized cotton

fabrics and were exposed to solar and UV irradiation to corroborate the antibacterial properties of the synthesized materials.

Materials and methods

Materials

Commercial lab coat (100% cotton, 244 g/m²) and Indiolino (100% cotton, 175 g/m²) fabrics were used as model textiles. Titanium isopropoxide (C₁₂H₂₈O₄Ti, 98%), glacial acetic acid (CH₃COOH, 98%), titanium chloride (TiCl₄, 98%) and titanium butoxide (Ti(OBu)₄, 98%) were provided by Sigma-Aldrich and used without further purification. Before the treatments, the fabrics were washed with a non-ionic detergent and dried for 24 h at 70 °C. All impregnation procedures were carried out using 5 cm × 5 cm of cotton squares.

Synthesis and incorporation of TiO₂-NPs on cotton fabrics

Modified cotton fabrics were obtained from three synthesis methods of TiO₂-NPs, in each one the preparation method was improved varying the synthesis parameters, such as: loading of Ti precursor, treatment and synthesis temperature, reaction time and washing conditions.

Sonochemical synthesis

The TiO₂-NPs impregnation on cotton fibers by sonochemical synthesis was carried out according to the methodology proposed by Akhavan et al. (2014) and Montazer and Seifollahzadeh (2011) and it was adapted according to our purposes. Briefly, the TiO₂ nanocrystals were synthesized and simultaneously impregnated on cotton fabrics under ultrasonic irradiation by hydrolysis of titanium isopropoxide (IPT) in the presence of distilled water, using acetic acid as hydrolysis catalyst. In a typical preparation, distilled water and glacial acetic acid were placed in a flask, then the solution was stirred for 5 min at room temperature (RT). Subsequently, a 5 × 5 cm of cotton piece was immersed into the solution and the flask was placed in an ultrasonic bath (Brason 2200; 50 kHz, 220 W) for 5 min at RT. Afterwards, 1 mL of IPT was added dropwise to the solution in the bath and the temperature was increased to 65 °C and kept constant for 4 h. After the reaction time, the flask was removed from the ultrasound bath and the cotton squares were dried

at RT in a desiccator for 24 h. The fabrics were washed with distilled water and dried at 70 °C for 24 h.

Hydrothermal synthesis

The cotton samples were first dried at 70 °C for 4 h to remove adsorbed water and immediately dipped for 12 h into a 1 wt.% solution of titanium butoxide (BuOT) in a mixture of tertbutanol and acetic acid (90/10 wt.%). Samples were then removed and dried at 60 °C for 2 h in an oven, to evaporate the solvent, and then transferred into a 200 mL Teflon-lined stainless steel autoclave, half-full of water, which was then placed in an oven maintained at the required temperature (i.e. 110 °C) for the hydrothermal treatment during 3 h. Finally, samples were dried at 50 °C for 2 h (Abid et al. 2016).

Solvothermal synthesis

The procedure for the synthesis of TiO₂ nanomaterials (Wu et al. 2007) was adapted to obtain NPs-TiO₂ on the cotton samples by solvothermal method as follows, a certain volume of TiCl₄ (1.0–9.0 mL) was quickly dropped into a fixed volume of acetone (60 mL) under vigorous stirring at RT. The obtained solution and cotton fabrics were transferred to a Teflon-lined autoclave and sealed. The autoclave was then placed in an oven for solvothermal treatment at 100 °C for 12 h. After cooling at RT, the cotton fabrics were removed, washed several times with acetone and finally dried at 50 °C for 2 h.

The nomenclature used for the synthesized materials is shown in Table 1, where commercial fabrics were labeled according to the cotton fabric (I or C for Indiolino or Cotton lab coat, respectively), Ti precursor (I, B and T for IPT, BuOT or Ti chlorine, respectively) and the method used (U, S or H; for sonosynthesis (ultrasound), solvothermal or hydrotreated method, respectively). The synthesis temperature, the reaction time and the Ti loading (for selected samples, with best performance) are included as reference in Table 1.

Table 1 Nomenclature of the synthesized materials

	Fabric	Method	Precursor	Time (h)	Temperature (°C)	Ti (wt.%) [*]
IU	Indiolino	Sonosynthesis	IPT	4	65	2.7
IBH	Indiolino	Hydrothermal	BuOT	3	110	2.8
CIU	Cotton lab coat	Sonosynthesis	IPT	4	65	2.6
CBH	Cotton lab coat	Hydrothermal	BuOT	3	110	2.4
CTS	Cotton lab coat	Solvothermal	TiCl ₄	12	100	n.d

^{*}Evaluated by SEM-EDS

Photocatalytic tests

Methylene blue degradation tests using UV radiation

The photocatalytic properties of the TiO₂-NPs functionalized cotton samples were analyzed based on the methylene blue (MB) degradation, which was previously impregnated on the surface of the cotton fabrics. The cotton samples were cut into 2.5 cm × 2.5 cm squares and were impregnated with a MB solution (3 mL, 5 ppm). Then, the fabrics were exposed to UV-light source (320 nm) with an intensity of 3.5 mW/cm². The MB degradation was followed by UV-Vis DRS of the fabric squares at 0, 15, 30, 60 and 120 min of UV-light exposure. The maximum absorbance value (C₀) was determined by UV-Vis DRS spectroscopy. Meanwhile, the UV-Vis DRS absorption spectra of the fabrics containing MB were obtained at 0, 15, 30, 60 and 120 min of UV-light exposure. The rate of dye decomposition was calculated and compared based on the C/C₀ values, where C₀ and C represent the initial MB concentration on the impregnated cotton pieces and the MB concentration at the time *t*, respectively (Pakdel and Daoud 2013).

Methylene blue degradation tests using solar radiation

The photocatalytic degradation of MB using TiO₂-NPs functionalized cotton fabrics were also assessed using solar irradiation, in similar procedure to UV irradiation, before described. In this case, the cotton samples were placed in a container and then exposed to sunlight. The average natural day light irradiation intensity was 4 mW/cm², in winter from 9 am to 3 pm in Mexico City.

Antibacterial tests

Cell culture

For the bactericidal tests of the fabrics impregnated with TiO₂-NPs, *Escherichia coli* (MC4100) and *Bacillus pumilus* (B-41243) strains were used, which are gram-negative and gram-positive bacteria, respectively. *Escherichia coli* is a

gram-negative bacterium, rod shaped (2.0–6.0 μm in length) bacteria with rounded ends (Conti and Gettner 1962; Percival et al. 2014). *Bacillus pumilus* is a gram-positive bacterium, rod shaped (0.5–10 μm length) bacteria (Borsa et al. 2016; Grutsch et al. 2018). A freshly bacterial culture was prepared for each of the bacteria to study the bacterial activity of the samples. From an overnight culture of *E. coli* and *B. pumilus*, 900 μL were taken and added to 45 mL of fresh LB medium. Then the bacterial mediums were incubated using a New Brunswick Scientific G-25 Incubator Shaker, at 150 rpm and 37 $^{\circ}\text{C}$, until their optical density reached 0.1 at 600 nm ($\text{OD}_{600} = 0.1$). The optical density of the bacterial culture was measured using a Thermo Multiskan GO spectrophotometer at 600 nm.

Bactericidal activity of TiO_2 -NPs on fabrics

To study the bacterial activity, 4 μL of fresh bacteria culture was placed on squares fabrics of 0.5×0.5 cm. Then, the fabric pieces inoculated with bacteria were exposed to UV radiation (254 nm) using an Air Science UV-Box decontamination chamber. The fabrics were irradiated with UV light (254 nm) for 2.5 and 5 min on both sides. Subsequently, the cloth samples were incubated in petri dishes with LB agar for 18 h at 37 $^{\circ}\text{C}$ to study antibacterial activity.

Bactericidal in-situ study by SEM

After the samples were incubated, the antibacterial activity was analyzed by SEM Hitachi SU3500. The samples were dried at RT and placed on a sample holder using carbon tape. Then, the samples were analyzed at low vacuum conditions (25 Pa) and 7 kV. The images were taken at different magnifications (47X, 270X, 370X, 2000X and 3000X) and recorded digitally.

Washing tests

The cotton pieces were subjected to several washing cycles to determine the leaching of the TiO_2 -NPs. The washing cycles were carried out according to the textile standard FZ/T 73,023–2006 as follow: the cotton fabrics impregnated with TiO_2 -NPs were immersed in an ultrasound device (100 Hz) at 40 $^{\circ}\text{C}$ for 5 min. The washed cotton fabrics were removed and rinsed with distilled water. Afterwards, the cotton pieces and the washing water were analyzed by UV–Vis DRS and UV–Vis spectroscopy (respectively) to determine the amount of TiO_2 -NPs leached (Akhavan et al. 2014).

Characterization

Attenuated total reflectance infrared spectroscopy (ATR-FTIR) was carried out in Nicolet 6700 FTIR spectrometer

to corroborate the formation and successfully impregnation of TiO_2 -NPs on the cotton fabrics. Raman spectroscopy and D_xR Raman microscope Thermo Scientific was used to corroborate the surface characteristics of the materials. The synthesis solutions and the water from the washing tests were analyzed by UV–Vis spectroscopy at RT (Varian Cary 50) from 200 to 1100 nm to assess the impregnated Ti amount and the leached Ti amount, respectively. Scanning electron microscopy (SEM) coupled to energy dispersive spectroscopy (EDS) system was carried out using a Jeol JSM-5900 LV microscope to the morphological and elemental analysis. Surface area of cotton samples was determined using N_2 adsorption–desorption isotherms at –196 $^{\circ}\text{C}$ on a Tristar Micrometrics apparatus; the samples were degassed 8 h in vacuum at 350 $^{\circ}\text{C}$. Tensile strength of the samples chemically treated and without treatment were tested on a Digital traction force Gauge, LZKW. The MB degradation on the surface of the cotton pieces was analyzed by UV–Vis diffuse reflectance spectroscopy (UV–Vis DRS) by a Perkin Elmer Lambda 365.

Results and discussion

SEM–EDS micrographs and elemental mapping

All fabrics were analyzed by SEM–EDS. It is important to note that to obtain nano size particles, an optimum Ti loading should be immobilized on the cotton fabrics so as not to lose Ti species in the washing process by leaching. The cotton fabrics shown in Table 1 have an optimum Ti loading and, therefore only the highest Ti loading samples showed SEM–EDS signal due to the sensibility of the technique. Since those nano particles would only be observed appropriately by the TEM. Therefore, the SEM technique helped to select the optimum Ti loading corresponding to NPs domain (reported in Table 1).

Figure 1 shows the micrographs and elemental mapping of selected impregnated cotton fabrics. Figure 1a corresponds to the impregnated lab coat fabrics by sonochemical method (CIU) at 100X resolution. From Fig. 1a can be suggested the correct synthesis method since the observed size of TiO_2 corresponds to the NPs domain. Figure 1b shows the micrograph at 1000X resolution and it can be observed that the cotton threads are covered by TiO_2 -NPs (white dots) with an adequate particle size distribution on the cotton surface as it was also observed in Fig. 1a. Figure 1c shows the micrograph of cotton fabric without supported TiO_2 -NPs. Figure 1d shows the elemental mapping of Ti, confirming the adequate Ti distribution on the cotton fabric. For comparison purposes, Fig. 1e and 1f show a sample with high Ti loading than the cotton fabric shown in Fig. 1a and 1b. Both micrographs shown the microparticles domain of these

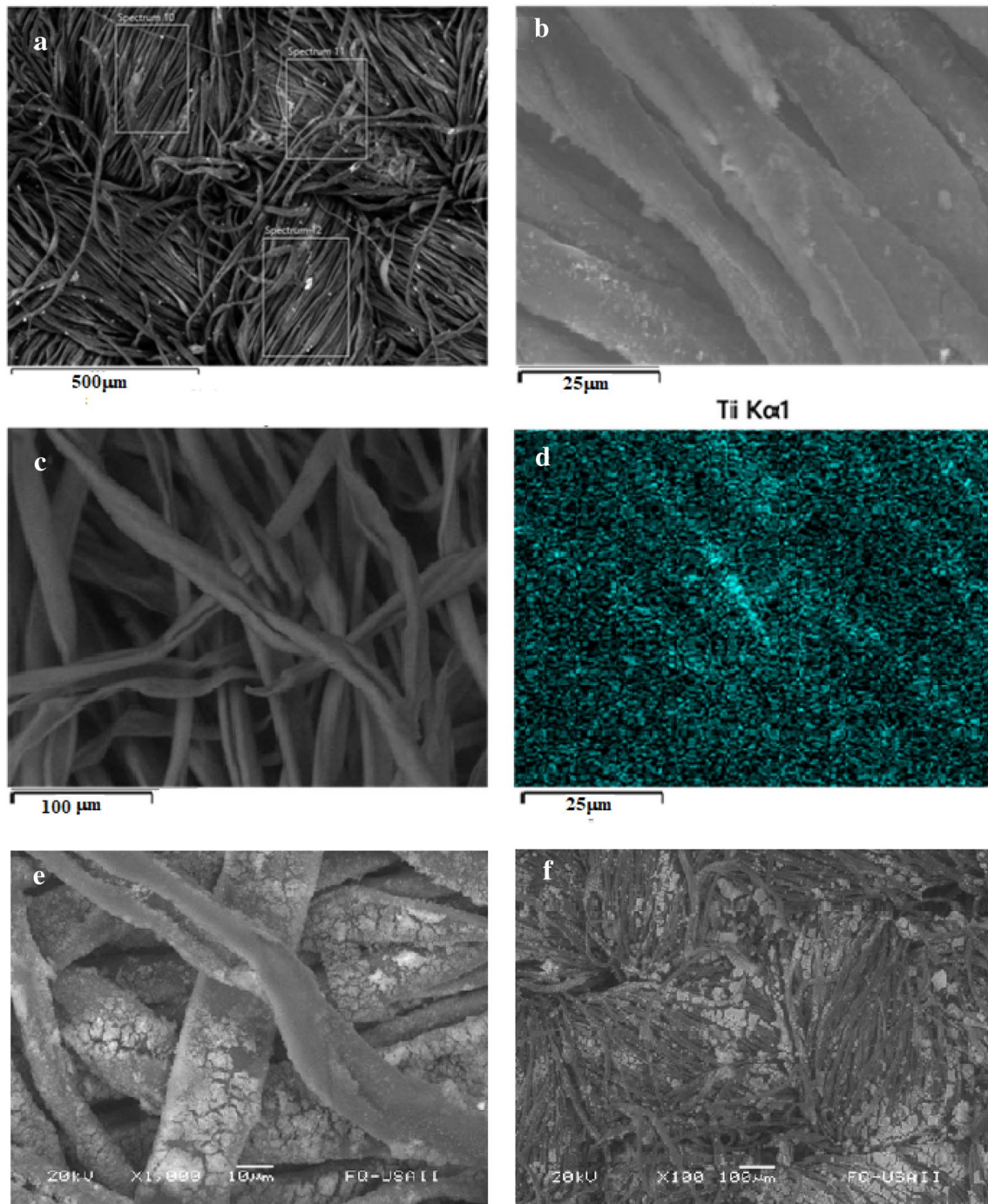


Fig. 1 Micrographs and elemental mapping of CIU (a–d) and fabrics with high Ti loading (e and f)

samples with high Ti loading. Similar results (not shown) were obtained for all fabrics.

Tensile and textural properties of fabrics

The Table 2 shows the surface area determined by N_2 physisorption, the lattice thread diameter, the grammage and the

tensile strength of the cotton fabrics. The tensile strength of the fabrics was assessed using the bare cotton fabrics and after a first and a second treatment. The surface area of the cotton fabrics is too low, less than $1 \text{ m}^2 \text{ g}^{-1}$, which is a typical value for cotton fabrics. Also, due to this low value of surface area, the immobilization of the TiO_2 -NPs should be carried out in a proper way to avoid TiO_2 -NPs leaching

Table 2 Tensile properties of the cotton fabrics

	Surface area (m ² /g)	Lattice thread diameter (mm)	Grammage (g/m ²)	Tensile strength of bare cotton fabrics (N)	Tensile strength after 1st treatment (N) ^a	Tensile strength after 2nd treatment (N) ^b
Indiolino	0.4	0.38	175	9.90	15.22	13.82
Lab coat	0.6	0.30	244	8.33	10.39	9.21

^a1st treatment: ultrasound for 2 h and dried for 24 h at 65 °C

^b2nd treatment: ultrasound for 5 h and dried for 24 h at 110 °C

due to the saturation of OH- surface groups on the cotton fabrics. According to the previous SEM–EDS results, the morphological characteristics suggested that TiO₂-NPs was successfully synthesized and as will be seen later, the immobilization of TiO₂-NPs was carried out satisfactorily.

The lattice thread diameter of lab coat and Indiolino is very similar, the difference is only 0.08 mm, which indicates the great similarity of both cotton-derived fabrics. Also, this feature explains in great manner the low value of surface area since the cotton fabrics are made up of intertwined threads. Additionally, the thin structure of the cotton fabrics threads emphasizes that their surface can only be coated by very small structures such as nanoclusters or nanoparticles. The grammage represents the cotton fabric weight per unit area and as it can be observed, its value is greater for the lab coat cotton than for Indiolino. The grammage value difference is due to the density values that are slightly different due to the final preparation of the fabrics. Therefore, it could be inferred that lab coat cotton fabrics present a greater interaction with TiO₂-NPs on their surface. The tensile strength of the cotton fabrics, without and with ultrasound treatments, is an important characteristic since the immobilization of TiO₂-NPs could largely depend on this property. That is, in addition to the fact that TiO₂-NPs immobilization on the cotton fabrics surface is a function of physisorption and to the chemisorption phenomena, probably TiO₂-NPs interaction with OH- surface groups could also be influenced by the mechanical stability of the intertwined threads of cotton fabrics. Breaking loads of Indiolino and Lab coat fabrics were 9.90 and 8.33 N, respectively. After first treatment (the immersion of cotton fabrics in an ultrasound bath for 2 h and then a drying process at 65 °C), the fabrics were about 54 and 25% more resistant than the pristine one. The acidic condition of reaction solution (pH = 3.5) and ultrasonic irradiation did not cause destruction on the structure of cotton. After the second treatment (the cotton fabrics were maintained for 5 h under ultrasound irradiation and finally a dried process at 110 °C), the fabrics were about 10% less resistant than fabrics with only one first treatment but were more resistant than untreated fabrics. This loss on tensile strength fabric could be related to the ultrasonic irradiation and/or cleavage of the cellulosic chains

by acid hydrolysis (Akhavan et al. 2014). In addition, shrinkage might occur while sonication causing a slight increase in breaking elongation from 5 to 6%. The results indicated that in-situ sonosynthesis of TiO₂-NPs on the cotton fabric did not cause any significant damage to on the structure of cotton, as has also been stated by Akhavan et al. (2014).

In contrast, the fabric prepared by solvothermal method (CTS) from TiCl₄ at 100 °C in the autoclave produces HCl. Therefore, strong acidic condition of reaction solution provokes the destruction of the structure of cotton. Even neutralizing the acid conditions, was not possible to preserve the structure of cotton and this preparation method was discarded.

Raman spectroscopy

Cotton fibers are composed of the biopolymer β -cellulose (Fig. 2), whose repeating units are β -D-glucose molecules and are linked by β -1,4-glucoside bonds (Pakdel and Daoud et al. 2013). Its fibers have a great amount of hydroxyl groups on the cellulose surface, so that extensive research have been made about the chemical functionalization of this material taking advantage of this high reactive functional group (OH-). The reactivity of cotton is a function of the considerable number of hydroxyl groups located on the C2, C3 and C6 carbons in each β -D-glucopyranose or anhydroglucose unit (Pakdel and Daoud 2013; Al-Taweel and Saud 2016).

Al-Taweel and Saud (2016) stated that the TiO₂-NPs can interact strongly with surface hydroxyl and carboxyl groups of cotton cellulose. Additionally, Pakdel and Daoud

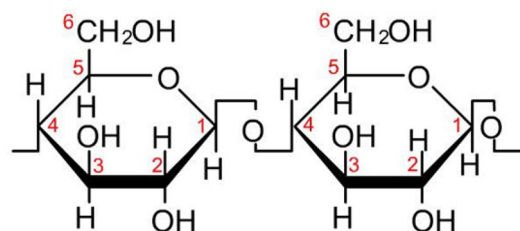


Fig. 2 β -D-glucose molecules

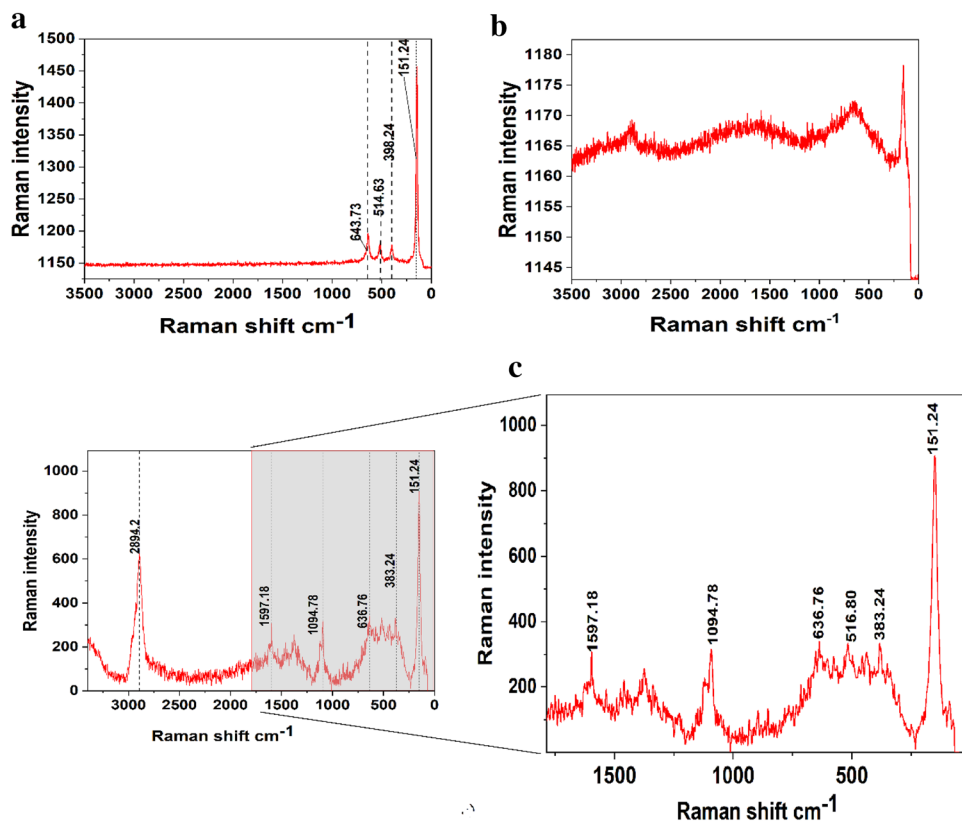
(2013), Daoud and Xin (2004) and Daoud et al. (2005) propose an anchoring mechanism for TiO₂/SiO₂ composites on the cotton surface where nanoparticles are anchored on the hydroxyl groups of the C2, C3 and C6 carbons in cellulose. Therefore, it can be suggested that TiO₂-NPs synthesized and immobilized by ultrasonic irradiation as in this work, could be anchored on the surface of cotton fabrics in a similar way as commented above. In this sense, the Fig. 3 shows the Raman spectra of Degussa P25, IIU and CIU. From Fig. 3a it can be observed the strong absorption at 151 cm⁻¹ (Eg) corresponding to the vibrational mode of anatase TiO₂ NPs and less intense bands at 398 cm⁻¹ (B1g o A1g and B1g), also for this phase. The bands at 514 cm⁻¹ (Eg) and 643 cm⁻¹ (A1g) are assigned to rutile phase of TiO₂, according to Qina et al. (2009), Burlacov et al. (2006) and Hana et al. (2018). The observed red shift for the bands is because the increase of crystallinity of the sample and, also could be by the interaction of anatase and rutile TiO₂ phases.

The observed bands at 1094, 578, 516, 433 and 383 cm⁻¹ for CIU (Fig. 3c) corresponding at vibrational modes of cellulose. According with Abid et al. (2017), the most intense band at 1094 cm⁻¹ could be assigned to the C–O–C symmetric and asymmetric stretching mode of the glycosidic bonds of the cellulose's glucopyranose ring. Figure 3c shows the vibrational modes at 144, 151, 383, 516, 513 and 638 cm⁻¹, which are characteristics to TiO₂-anatase nanoparticles, in agree accordance with

published literature (Al-Taweel and Saud 2016). These bands are assigned to the extension of the Ti–O bond (Eg) at 639 cm⁻¹, the bending of the Ti–O bond (A1g + B1g) at 517 cm⁻¹ and the bending of the O–Ti–O bond (Eg) at 397 cm⁻¹. It can be observed a red shift in the Eg mode frequencies for the TiO₂-NPs supported on the cotton fabrics, i.e., the band at 151 cm⁻¹ for the supported TiO₂-NPs (see Fig. 3c) correspond to the red shift of the band at 145 cm⁻¹ for TiO₂-anatase nanoparticles.

According to Abid et al. (2017), the red shift could be attributed to the phonon confinement effect due to the minor size of the TiO₂-NPs and the crystallinity increase. Even, the interaction between TiO₂-NPs and -OH groups on the cotton fabric could contributed to this effect. For Indiolino prepared by ultrasound irradiation (IIU) (Fig. 3b) it can be observed an intense band at 152 cm⁻¹ and less intense bands at 650 cm⁻¹, 1741 cm⁻¹, 2913 cm⁻¹. The first two bands could be related to anatase TiO₂-NPs and the bands at 1741 cm⁻¹, 2913 cm⁻¹ could be assigned to the characteristic vibrational modes of cellulose and TiO₂ phases. As for CIU, the red shift in the IIU Raman spectrum can be explained by the minor size of the TiO₂-NPs and/or the interaction between surface -OH groups of cotton fabrics and TiO₂-NPs. From these results, for both IIU and CIU, the presence of TiO₂-NPs intense bands allows to suggest the adequate functionalization of the cotton fabrics.

Fig. 3 Raman spectra of **a** Ti Degussa P25, **b** Indiolino prepared by ultrasound irradiation (IIU) and **c** cotton lab coat prepared by ultrasound irradiation (CIU)



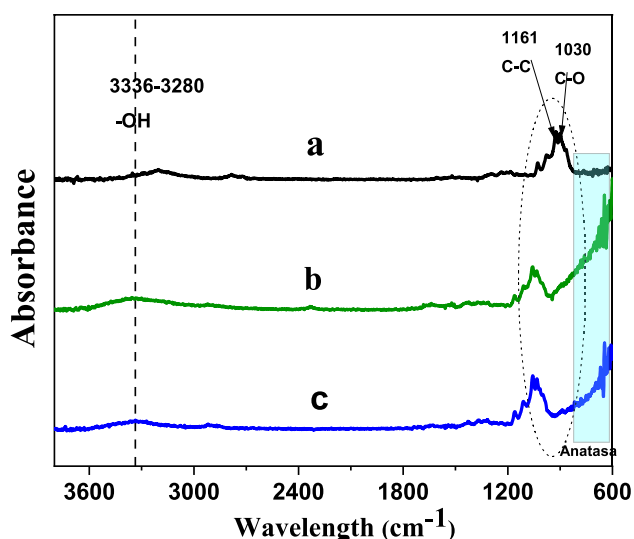


Fig. 4 FTIR-ATR spectra of: **a** cotton fabric, **b** CIU without washing, and **c** CIU after 5 washing cycles

Attenuated total reflectance infrared spectroscopy (FTIR-ATR)

Figure 4 shows the FTIR-ATR spectra of the cotton lab coat fabric and CIU. The bands at 1161 and 1030 cm^{-1} correspond to the tension vibration of the functional groups C–C and C–O of cellulose, respectively. For all samples, a broad band between 3336 and 3280 cm^{-1} is observed, which is characteristic of O–H functional groups in cellulose (Ugur et al. 2010).

These bands, characteristic of cellulose and observed in cotton fabric, persistent in CIU without and with washing treatment showing that the textile was not modified appreciably. Only was observed to shift of these bands to high wavelengths values, it could be attributed to the interaction of TiO_2 -NPs to cotton surface.

From 800 cm^{-1} toward longer wavelength, it can be observed the evolution of a broad region. According to Praveen et al. (2014) the region from 1000 cm^{-1} to 400 cm^{-1} correspond to the Ti–O stretching and Ti–O–Ti bridging stretching modes of the TiO_2 -NPs. Also, it is reported that around 450 cm^{-1} presents absorption band which is attributed to the TiO_2 NPs. The lack of definition in Fig. 4 below 800 cm^{-1} is due to FTIR-ATR was carried out with a diamond crystal with a range 4000–550 cm^{-1} , which does not allow a good definition of this region. However, the obtained results allow to establish the presence of TiO_2 -NPs (crystalline TiO_2 -anatase phase) on the cotton fabric surface. Figure 4 shows the FTIR-ATR spectra of the CIU before and after washing processes (Fig. 4b–c). As reference, the spectrum of the alone cotton fabric is shown (Fig. 4a). It can be observed that the FTIR-ATR spectrum of the cotton fabric

alone does not show the increasing absorption band below 800 cm^{-1} , which allowed to corroborate that this region can be attributed to the presence of TiO_2 -NPs.

UV–Vis spectra of reaction and washing solutions

Figure 5 shows the UV–Vis spectra of the preparation and washing solutions of the synthesized fabrics. TiO_2 spectrum presents an absorption band at ~ 270 – 280 nm and therefore it is possible the identification of the TiO_2 -NPs in the preparation and washing effluents (Akhavan et al. 2014). It is important to note that TiO_2 -NPs physically adsorbed on the fabric surface are likely to leach into the washing solution. The spectrum of CIU prepared with an excess of IPT and the CIU prepared with an adequately amount of IPT are shown in Fig. 5 (a and b, respectively). The CIU prepared with an excess of IPT showed the greatest absorbance of the all analyzed samples. The UV–Vis spectrum of CIU prepared with an adequately amount of IPT shown an absorption band around of ~ 270 – 280 nm, which is less intense than the sample with an excess of IPT. CBH, IBH and IIU samples showed even lower values of absorption. Also, the UV–Vis analysis of subsequent washing solutions showed no absorption bands suggesting that the TiO_2 -NPs do not leach from the fabric surface. The above results indicated that the good immobilization of TiO_2 -NPs on the cotton fibers.

It is important to mention that TiO_2 -NPs could be anchored on hydroxyl and/or carboxyl groups by covalent linkages (Akhavan et al. 2014). The chemically anchored TiO_2 -NPs on the hydroxyl and carboxyl groups of the cotton surface must be the preponderant species that persist after

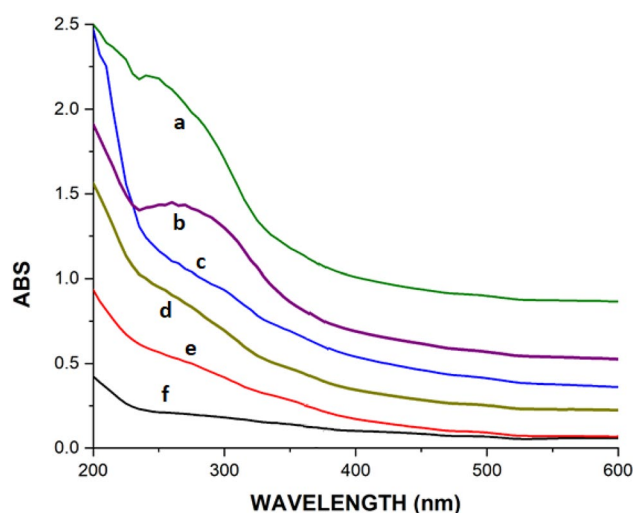
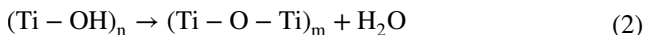
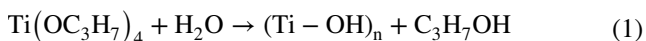


Fig. 5 UV–Vis spectra of washing effluents: **a** CIU prepared with excess of IPT, **b** CIU, **c** CBH, **d** IBH, **e** IIU and **f** water solution as reference

the washing tests, in agreement with Akhavan et al. (2014) and Montazer and Seifollahzadeh (2011).

According to Ugur et al. (2010), the simultaneous synthesis of TiO₂-NPs and the functionalization of cotton fibers in a one-step process by sonochemical irradiation can be represented by a hydrolysis reaction (Eq. 1) and a condensation reaction (Eq. 2) as follow:



The formation of TiO₂-NPs can be explained in two steps as follow: 1) The hydrolytic Ti species, formed by the IPT hydrolysis in water, are condensed in many gel nuclei units and then are aggregated in large clusters. 2) The ·OH and ·H radicals, formed by the water sonolysis due to the cavitation process by the ultrasound irradiation, promote the hydrolysis of IPT and the polycondensation of Ti–OH groups, generating the TiO₂-NPs. According to Ugur et al. (2010), the sonochemical formation of TiO₂-NPs is carried out in the liquid phase, around the collapsing bubble and not within the collapsing cavity. The TiO₂-NPs generation is a function of the microturbulence and the shock waves. The microturbulence is due to the radial liquid movement by the cavitation of the bubbles. The shock waves are a result of the high-pressure waves emitted by collapsing bubbles. The conjunction of microturbulence and the shock waves phenomena generates a localized heat and pressure transient zones. Large temperature and pressure gradients cause water sonolysis, therefore ·OH and ·H radicals are generated and promoting the Ti–OH condensation. It is proposed that nucleation ratio increases

by the shock waves and the growth rate of the nanocrystals is a function of the microturbulence.

Photocatalytic activity

The photocatalytic activity of the TiO₂-NPs on cotton fabrics was assessed to corroborate the self-cleaning properties and the antiviral and antibacterial features. Since as it has been established the ROS generation is a key factor. In this sense, the photocatalytic degradation of model molecules such as dyes has been carried out as elsewhere (Hosseini-Sarvari et al. 2022; Skiba and Vorobyova 2020). In this sense, 5 × 5 cm squares of the fabrics were impregnated with MB (methylene blue) solution (10 ppm) and subsequently irradiated with UV (320 nm) or solar irradiation. The adsorbed amount of MB did not exceed 5% for all cotton samples, which is indicative of the low adsorption capacity of the material, due mainly to the low surface area of the materials (see Table 2). Due to the characteristic blue color of the Indiolino cotton fabric it was not possible to determine the MB degradation by DRS. For this reason, white color cotton indiolino was used for the photodegradation tests. Prior to irradiation, the 5 × 5 cm squares were cut off in four parts (2.5 × 2.5 cm) and were placed in a set-up in such a way that all samples were irradiated with the same intensity. Further, the set-up was stored in the darkness for 1 h to discard any possible change in the concentration, resulting from the photolysis process (Abid et al. 2016). Figure 6 shows the MB degradation on IBH under solar (Fig. 6b to 6e) and under UV irradiation (Fig. 6g to 6j). It can be observed a noticeable decrease of the blue color on the cotton fabrics after UV and solar irradiation. The discoloration observed was due

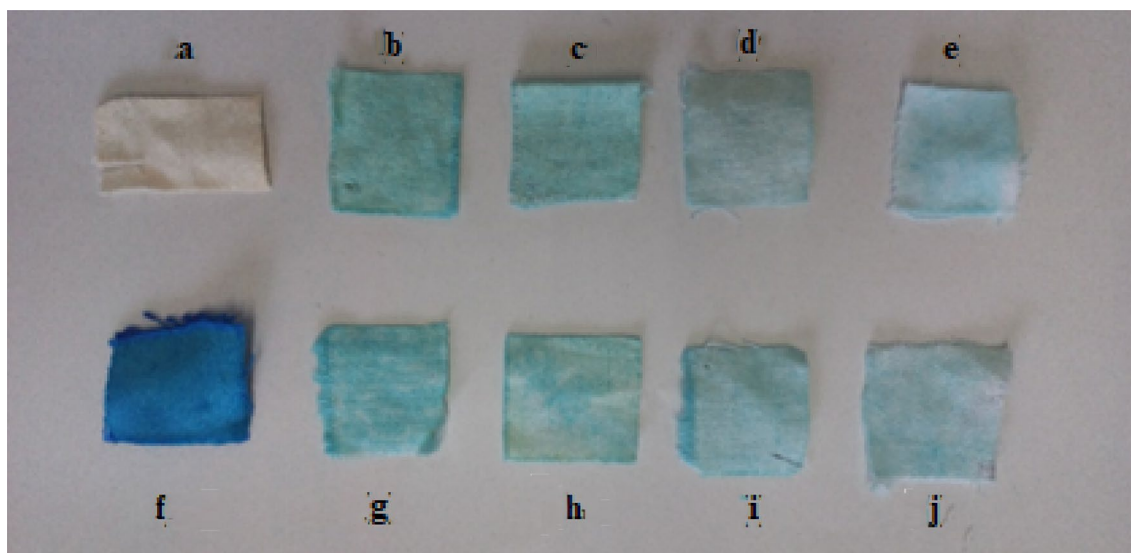


Fig. 6 MB degradation on IBH samples under solar irradiation (b to e; at 15, 30, 60 and 120 min, respectively) and under UV irradiation (g to j; at 15, 30, 60 and 120 min, respectively). a bare IBH and f IBH impregnated with MB solution

to the photocatalytic degradation of MB by the TiO₂-NPs presence, showing the efficiency of the functionalized cotton fabrics.

Also, the changes of the MB concentration on the fabrics were determined by UV–Vis DRS absorption at 0, 15, 30, 60 and 120 min of light exposure. According to Uddin et al. (2007), the observed band at 664 nm is assigned at dimeric and trimeric MB species adsorbed on the surface. The MB degradation was determined as the total MB conversion, by the C/C_0 relationship. Figure 7 shows the MB degradation, using IBH under UV irradiation in the photoreactor. It can be observed that MB was degraded almost 70% in 60 min. It is important to mention that the MB degradation of CIU (not shown) was near to 99% in 60 min under UV irradiation. Also, it was observed negligible change in the MB concentration in the presence of bare cotton fabric under UV or solar irradiation, which confirmed the effective role of the TiO₂-NPs in the photocatalytic activity. Based on these results it is possible to infer that IPT is a better option as Ti precursor than BuOT.

The MB degradation data were well fitted with a pseudo-first order kinetics. Table 3 shows the kinetic results of MB degradation using the lab coat and Indiolino fabrics prepared by sonochemical or hydrothermal methods. Under UV irradiation, for the fabrics synthesized by different method and Ti precursor, it can be observed that pseudo-first order kinetic constants for Indiolino fabrics (IBH and IIU) are higher than for the cotton fabrics (CBH and CIU); 0.01 vs. 0.0067/min and 0.0117 vs. 0.0075 cm⁻¹ (respectively).

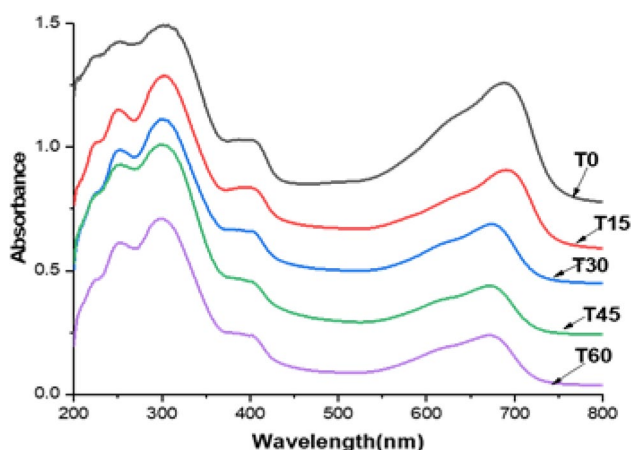


Fig. 7 DRS results of MB degradation on IBH, obtained by UV irradiation

Meanwhile, the pseudo-first order kinetic constants under solar irradiation are higher for Lab coat than Indiolino fabrics. The kinetic constants are: 0.0165 for CIU vs. 0.0142 for IIU and 0.0154 for CBH vs. 0.0117 for IBH.

The higher pseudo-first order kinetic constants values for Indiolino fabrics compared with cotton fabrics, under UV irradiation, probably could be because the lightly longer size of TiO₂ crystals for Indiolino fabrics, since as it has been stated the TiO₂ particles of larger size are more photoactive under shorter wavelengths, UV spectrum (Senić et al. 2011; Uddin et al. 2007). Contrarily, the higher photoactivity for cotton fabrics, under solar irradiation, it can be explained by two effects or by the combination of both. The first one could be due to the shorter size of TiO₂ crystals for cotton fabrics which could absorb longer wavelength photons, in visible spectrum. The second one could be due to the greater amount of the irradiated photons under solar irradiation. Figure 8 shows the MB degradation using CIU under sunlight irradiation. It can be observed that almost a complete MB degradation was achieved in 120 min. Additionally, the Table 3 show that the pseudo-first order kinetic constant for CIU under solar irradiation was higher than pseudo-first order kinetic constants for IBH and IIU (1.4 and 1.2 times, respectively). The aforementioned results confirmed the higher photoactivity of functionalized cotton lab coat fabrics compared to the functionalized Indiolino fabrics under solar irradiation.

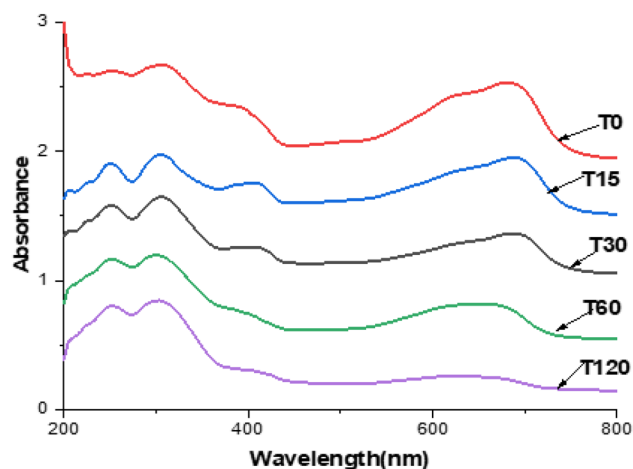


Fig. 8 DRS results of MB degradation on CIU, obtained by sunlight irradiation

Table 3 Kinetic results of MB photo degradation of NPs-TiO₂ on cotton fabrics by solar light (sun) or UV irradiation (uv)

	CIU sun	CIU uv	CBH sun	CBH uv	IBH sun	IBH uv	IIU sun	IIU uv
K (min ⁻¹)	0.0165	0.0075	0.0154	0.0067	0.0117	0.0100	0.0142	0.0117

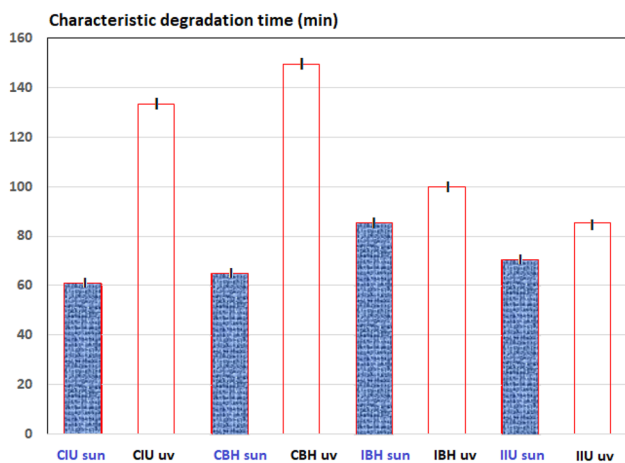


Fig. 9 Characteristic degradation time (τ) of MB for all synthesized cotton fabrics under UV or solar (sun) irradiation

The characteristic degradation time (τ) is the time needed to degrade half of the contaminant species present in the experiment. Figure 9 shows the τ of MB under UV or solar irradiations. For all samples (CIU, CBH, IBH and IBU), τ was reached faster under solar irradiation than under UV irradiation. That is, the same cotton fabric (cotton lab coat or Indiolino) prepared by the same method and Ti precursor and used under solar irradiation showed a greater MB degradation than when UV radiation was used on the same fabrics. These results are according to the reported pseudo-first order kinetic constants in Table 3 discussed earlier. This behavior could be due to the simultaneous effect of the shorter size of TiO_2 crystals for cotton fabrics (which absorb visible irradiation) and the greater amount of the irradiated photons under solar irradiation. In general, the functionalized cotton samples synthesized in this work shown an adequately structure and a successful photocatalytic behavior as has been discussed previously.

Bactericidal activity of TiO_2 -NPs on fabrics

The bactericidal activity of the fabrics synthesized was not possible to study by Kirby-Bauer technique because these ones do not form inhibition region, which has also been previously reported with fabrics impregnated with TiO_2 -NPs (Singhal et al. 2021). For this reason, fabrics squares of $0.5 \text{ cm} \times 0.5 \text{ cm}$ from IIU, IBH, CIU and CBH were inoculated with the *E. coli* bacteria and were evaluated in Petri dishes with LB-agar medium. After the inoculation without UV irradiation, it was found that the IIU sample, TiO_2 -NPs impregnated Indiolino fabric by sonosynthesis and using isopropoxide as Ti precursor, has a greater capacity to inhibit *E. coli*, (see Fig. 10, sample 1). Also, CIU showed good antibacterial capacity (sample 3). The fabrics prepared by hydrothermal method, IBH (sample 2) and CBH (sample

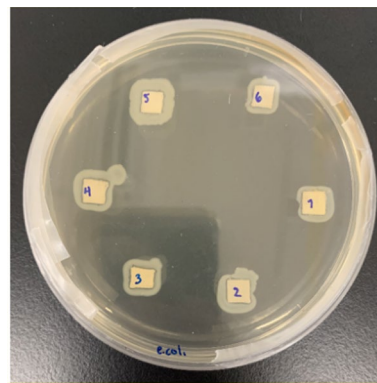


Fig. 10 Antibacterial activity of the fabrics on petri dish LB-agar. Sample 1: IIU, sample 2: IBH, sample 3: CIU, sample 4: CBH. Controls samples (5 and 6) correspond to cotton lab coat and Indiolino, respectively

4), showed the shorter bacterial inhibition capacity. It is important to note that Indiolino without TiO_2 -NPs (sample 6) showed bactericidal capacity, in a minor amount of its counterparts that contain TiO_2 -NPs. The halo of bacteria around the Indiolino fabric in sample 6 is more homogeneous than the other TiO_2 -NPs treated fabrics.

Based on the bactericidal results obtained in the Petri dishes, the *in-situ* antimicrobial activity analysis was carried out by SEM only for IIU sample and its corresponding control. The *E. coli* and *B. pumilus* bacteria was grown on the surface of the Indiolino fabric (control sample), which can be observed in the SEM micrographs in Fig. 11a and Fig. 11c. In both cases it was possible to observe the bacteria at 2000X magnification (see Fig. 11b y 11d and it can be observed that the bacteria cover most of the Indiolino surface. The *E. coli* (Fig. 11b) and *B. pumilus* (Fig. 11d) bacteria show no apparent damage, and it is observed a normal morphology and size, in agree with (Percival et al. 2014; Grutsch et al. 2018). In the case of TiO_2 -NPs treated Indiolino fabric, the bactericidal activity was significantly appreciated by means of SEM, see Fig. 12. Fig 12a, b show the fabrics at low magnification (1300X) where the homogeneous deposition of the TiO_2 and bacteria can be observed. In Figure b and Figure d, the bacteria *E. coli* and *B. pumilus* can be seen in greater detail (see insets). In both cases, the areas without TiO_2 -NPs showed the presence of bacteria, that is the bacteria grew in zones without TiO_2 deposits, which demonstrates the ability to inhibit both bacteria. When the samples are irradiated with UV irradiation for 2.5 min on both sides, it is possible to observe a greater bactericidal capacity on the fabric surface, see Fig. 13. The Fig. 13a shows the *E. coli* biofilm with abnormal morphology or damage. From Fig. 13b it can be observed that bacteria only grew on areas without NPs, as was analyzed for the other Indiolino fabrics. In the

Fig. 11 SEM micrographs of Indiolino fabric inoculated with *E. coli* (a) and *B. pumilus* (c). Micrographs at 2000X magnification for *E. coli* (b) and *B. pumilus* (d)

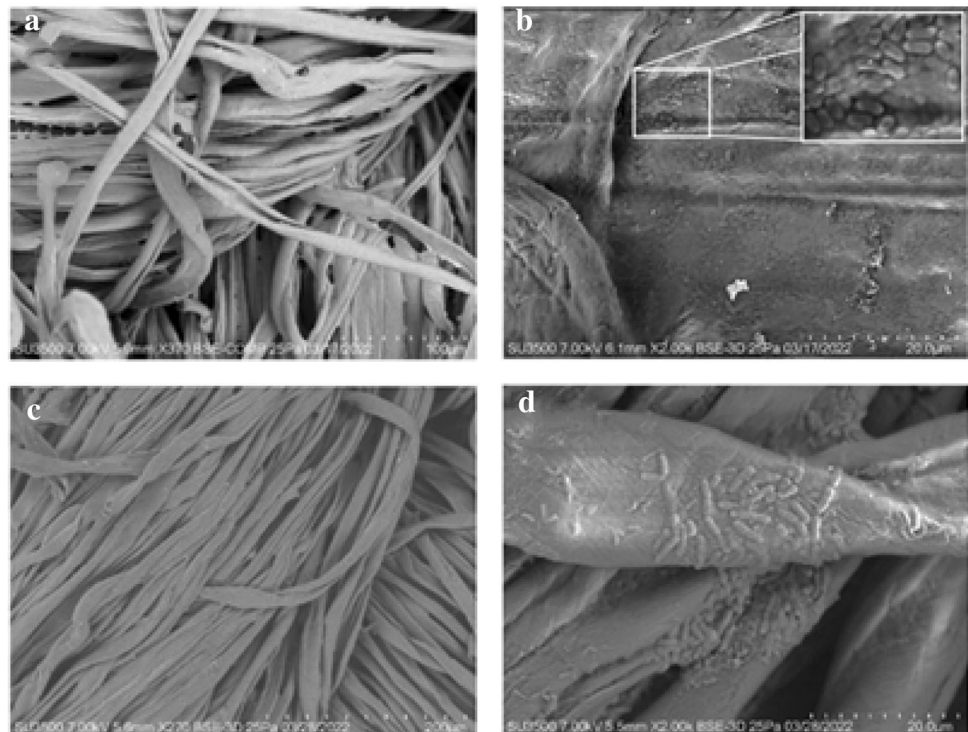
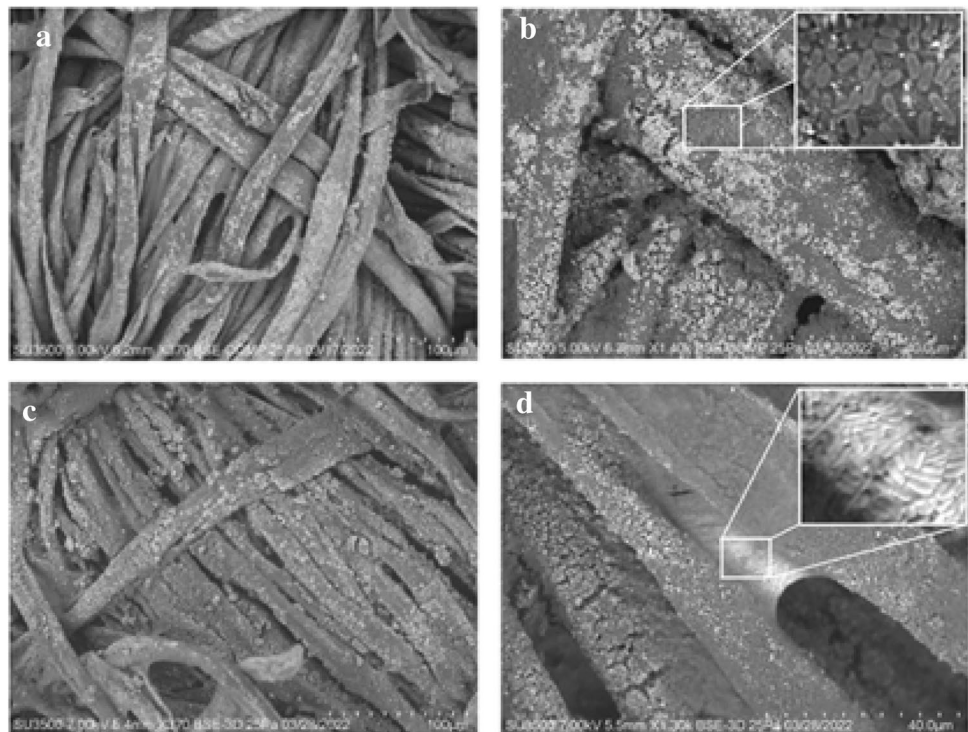


Fig. 12 SEM micrographs at 1300X of TiO₂-NPs treated Indiolino fabric and inoculated with *E. coli* (a) and *B. pumilus* (c). Micrographs at high magnification (> 1300X) for *E. coli* (b) and *B. pumilus* (d)



case of the fabric inoculated with *B. pumilus*, the bacteria were totally eliminated (see Fig. 13c) under UV irradiation. Additionally, bacteria were not found on the fabric surface, even the areas without NPs are free of bacillus. When the Indolino fabrics were exposed for 5 min on both

sides, both bacteria were no longer found in the fabric with and without TiO₂-NPs.

The IIU sample showed the best bactericidal capacity, which could be due to a better distribution of the NPs on Indiolino surface when the sonosynthesis method is used.

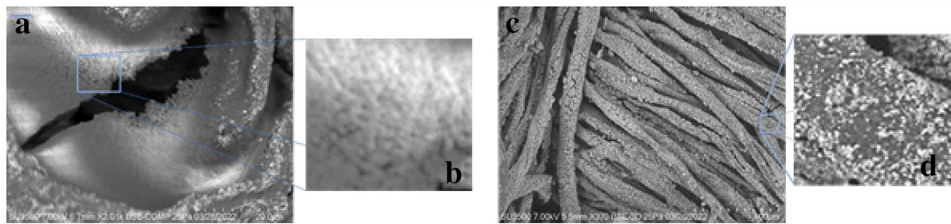


Fig. 13 SEM micrographs of treated TiO₂-NPs Indiolino fabric under UV irradiation for 2.5 min on both sides (5 min total), inoculated with *E. coli* (a) and *B. pumilus* (c). Micrograph magnifications of *E. coli* (b) and *B. pumilus* (d) on the Indiolino fabric

According to the *in-situ* SEM analysis, the better the nanoparticles are distributed, the greater the antimicrobial effect that results. Therefore, the homogeneity of the TiO₂-NPs on the surface fabric should be considered to have an efficient bactericidal capacity.

Conclusions

Titania nanoparticles (TiO₂-NPs) were successfully synthesized and simultaneously immobilized on cotton fabrics by several methods. The synthesis of TiO₂ anatase and its impregnation was confirmed by UV-Vis, SEM-EDX, Raman and FTIR-ATR spectroscopy.

The leaching of the TiO₂-NPs from the cotton fabrics after washing cycles was analyzed by UV-Vis and the characteristic band of anatase TiO₂-NPs was observed at a very low intensity suggesting the adequate impregnation of the TiO₂-NPs on the cotton fibers.

The TiO₂-NPs functionalized cotton fabrics degraded 99% of methylene blue in 60 min by photocatalysis under UV and solar irradiation confirming self-cleaning properties.

The bactericidal capacity of the impregnated TiO₂-NPs, determined by *in-situ* SEM analysis, against *E. coli* (gram negative) and *B. pumilus* (gram positive) was greater for Indiolino cotton. The TiO₂-NPs homogeneous distribution on the cotton fabric surface enhance the bactericidal capacity which is favored by the sonosynthesis method using Ti isopropoxide as precursor.

The results show that, it is feasible the functionalization of cotton fabrics with photoactive TiO₂-NPs to produce face masks with good bactericidal capacity and self-cleaning properties.

Acknowledgements We thank to H. Fabián Alonso-Cordero (UMAC-CICESE) for the SEM analysis, and Iván Puente (FQ-UNAM) for the SEM-EDS analysis.

Author contributions Conceptualization: SFM, LCC; LCC, Formal analysis: GAN, RDCN, SFM; Funding acquisition: SFM, LCC; Investigation: LCC, VMC, RDCN, KAHH; Methodology: LCC, VMC, RDCN, KAHH; Project administration: SFM; Resources: SFM;

Supervision: SFM; Validation: MAAA; Visualization: MAAA; Roles/ Writing—original draft: MAAA; Writing—review & editing: MAAA.

Funding This work was funded by the Dirección General de Asuntos del Personal Académico (DGAPA) of the Universidad Nacional Autónoma de México (UNAM) by the Research Support Program (PAPIIT, project IV100121).

Declarations

Conflict of interest On behalf of all authors, the corresponding author states that there is no conflict of interest.

References

- Abid M, Bouattour S, Conceição DS, Ferraria AM, Ferreira LJV, Botelho do Rego A. M, Vilarc MR, Boufi S, (2016) Hybrid cotton-anatase prepared under mild conditions with high photocatalytic activity under sunlight. RSC Adv 6:58957–58969. <https://doi.org/10.1039/C6RA10806G>
- Abid M, Ferraria BS, AM, Conceição DS, Carapeto AP, Ferreira LJV, Botelho do Rego AM, Chehimi MM, Vilar MR, Boufi S, (2017) Facile functionalization of cotton with nanostructured silver/titania for visible-light plasmonic photocatalysis. J Colloid Interface Sci 507:83–94. <https://doi.org/10.1016/j.jcis.2017.07.109>
- Akhavan F, Montazerb SM (2014) In situ sonosynthesis of nano TiO₂ on cotton fabric. Ultrason Sonochem 21:681–691. <https://doi.org/10.1016/j.ultsonch.2013.09.018>
- Al-Taweel SS, Saud HR (2016) New route for synthesis of pure anatase TiO₂ nanoparticles via ultrasound-assisted sol-gel method. J Chem Pharm Res 8:620–626
- Borsa BA, Aldağ ME, Tunalı B, Dinç U, Güngördü DZ, Özalp VC (2016) A sepsis case caused by a rare opportunistic pathogen: *Bacillus pumilus*. Mikrobiyol Bul 50:466–470. <https://doi.org/10.5578/mb.27575>
- Botequim D, Maia J, Lino MMF, Lopes LMF, Simões PN, Ilharco LM, Ferreira L (2012) Nanoparticles and surfaces presenting antifungal, antibacterial and antiviral properties. Langmuir 28:7646–7656. <https://doi.org/10.1021/la300948n>
- Burlacov I, Jirkovský J, Müller M, Heimann RB (2006) Induction plasma-sprayed photocatalytically active titania coatings and their characterisation by micro-Raman spectroscopy. Surf Coat Tech 201:255–264. <https://doi.org/10.1016/j.surfcoat.2005.11.117>
- Conti SF, Gettner ME (1962) Electron microscopy of cellular division in *Escherichia coli*. J Bacteriol 83:544–550. <https://doi.org/10.1128/jb.83.3.544-550.1962>

- Daoud WA, Xin JH (2004) Nucleation and growth of anatase crystallites on cotton fabrics at low temperatures. *J Am Ceram Soc* 87:953–955. <https://doi.org/10.1111/j.1551-2916.2004.00953.x>
- Daoud WA, Xin JH, Yi-He Z (2005) Surface functionalization of cellulose fibers with titanium dioxide nanoparticles and their combined bactericidal activities. *Surf Sci* 599:69–75. <https://doi.org/10.1016/j.susc.2005.09.038>
- Grutsch AA, Nimmer PS, Pittsley RH, McKillip JL (2018) *Bacillus* spp. as Pathogens in the Dairy Industry. In: Holban AM, Grumezescu AM (eds) *Handbook of Food Bioengineering, Foodborne Diseases*. Academic Press, Elsevier, pp 193–211
- Guo W, Lin Z, Wang X, G, (2003) Sonochemical synthesis of nanocrystalline TiO₂ by hydrolysis of titanium alkoxides. *Microelectron Eng* 66:95–101. [https://doi.org/10.1016/S0167-9317\(03\)00031-5](https://doi.org/10.1016/S0167-9317(03)00031-5)
- Hadad L, Perkas N, Gofer Y, Calderon-Moreno J, Ghule A, Gedanken A (2007) Sonochemical deposition of silver nanoparticles on wool fibers. *J Appl Polym Sci* 104:1732–1737. <https://doi.org/10.1002/app.25813>
- Hana E, Vijayarangamuthu K, Youn J, Parkb Y, Jung S, Jeon K (2018) Degussa P25 TiO₂ modified with H₂O₂ under microwave treatment to enhance photocatalytic properties. *Catal Today* 303:305–312. <https://doi.org/10.1016/j.cattod.2017.08.057>
- Hosseini-Sarvari M, Jafari F, Abdulhamid D (2022) The study of TiO₂/Cu₂O nanoparticles as an efficient nanophotocatalyst toward surface adsorption and photocatalytic degradation of methylene blue. *Appl Nanosci* 12:2195–2205. <https://doi.org/10.1007/s13204-022-02474-x>
- Hussain CM (2020) *Handbook of nanomaterials for manufacturing applications*. Elsevier
- Konda A, Prakash A, Moss GA, Schmoltd M, Grant GD, Guha S (2020) Aerosol filtration efficiency of common fabrics used in respiratory cloth masks. *ACS Nano* 14:6339–6347. <https://doi.org/10.1021/acsnano.0c03252>
- Lessan F, Montazer M, Moghadam MB (2011) A novel durable flame-retardant cotton fabric using sodium hypophosphite, nano TiO₂ and maleic acid. *Thermochim Acta* 250:48–54. <https://doi.org/10.1016/j.tca.2011.03.012>
- Militky J, Novak O, Kremenakova D, Wiener J, Venkataraman M, Zhu G, Yao J, Aneja A (2021) A review of impact of textile research on protective face masks. *Materials* 14:1937. <https://doi.org/10.3390/ma14081937>
- Montazer M, Seifollahzadeh S (2011) Enhanced self-cleaning, antibacterial and UV protection properties of nano TiO₂ treated textile through enzymatic pretreatment. *Photochem Photobiol* 87:877. <https://doi.org/10.1111/j.1751-1097.2011.00917.x>
- Ogunsona EO, Muthuraj R, Ojogbo E, Valerio O, Mekonnen TH (2020) Engineered nanomaterials for antimicrobial applications: A review. *Appl Mater Today* 18:100473. <https://doi.org/10.1016/j.apmt.2019.100473>
- Pakdel E, Daoud WA (2013) Self-cleaning cotton functionalized with TiO₂/SiO₂: Focus on the role of silica. *J Colloid Interface Sci* 401:1–7. <https://doi.org/10.1016/j.jcis.2013.03.016>
- Percival SL, Williams DW (2014) *Escherichia coli*. In: Percival SL, Yates MV, Williams DW, Chalmers RM, Gray NF (eds) *Microbiology of Waterborne Diseases*. Elsevier, Academic Press, pp 89–117
- Perelshtein I, Applerot G, Perkas N, Wehrschuetz-Sigl E, Hasmann A, Guebitz G, Gedanken A (2009a) Antibacterial properties of an in situ generated and simultaneously deposited nanocrystalline ZnO on fabrics. *Appl Mater Inter* 1:361–366. <https://doi.org/10.1021/am8000743>
- Perelshtein I, Applerot G, Perkas N, Wehrschuetz-Sigl E, Hasmann A, Guebitz G, Gedanken A (2009b) CuO–cotton nanocomposite: formation, morphology, and antibacterial activity. *Surf Coat Technol* 204:54–57. <https://doi.org/10.1016/j.surfcoat.2009.06.028>
- Perelshtein I, Applerot G, Perkas N, Grinblat J, Gedanken A (2012) A one-step process for the antimicrobial finishing of textiles with crystalline TiO₂ nanoparticles. *Chem Eur J* 18:4575–4582. <https://doi.org/10.1002/chem.201101683>
- Prasad K, Pinjari DV, Pandit AB, Mhaske ST (2010) Synthesis of titanium dioxide by ultrasound assisted sol–gel technique: Effect of amplitude (power density) variation. *Ultrason Sonochem* 17:697–703. <https://doi.org/10.1016/j.ultrsonch.2010.01.005>
- Praveen P, Viruthagiri G, Mugundan S, Shanmugam N (2014) Structural, optical and morphological analyses of pristine titanium dioxide nanoparticles – Synthesized via sol–gel route. *Spectrochim Acta Part A* 117:622–629. <https://doi.org/10.1016/j.saa.2013.09.037>
- Qina X, Jing L, Tian G, Qu Y, Feng Y (2009) Enhanced photocatalytic activity for degrading Rhodamine B solution of commercial Degussa P25 TiO₂ and its mechanisms. *J Hazard Mater* 172:1168–1174. <https://doi.org/10.1016/j.jhazmat.2009.07.120>
- Senić Ž, Bauk S, Vitorović-Todorović M, Pajić N, Samolov A, Rajić D (2011) Application of TiO₂ nanoparticles for obtaining self decontaminating smart textiles. *Sci Tech Rev* 61:63–72
- Singhal S, Khanna P, Khanna L (2021) Synthesis, comparative in vitro antibacterial, antioxidant and UV fluorescence studies of bis indole Schiff bases and molecular docking with ct-DNA and SARS-CoV-2 M^{pro}. *Luminescence* 36:1531–1543
- Skiba M, Vorobyova V (2020) Synthesis OF AG/TiO₂ nanocomposite via plasma liquid interactions and degradation methylene blue. *Appl Nanosci* 10:4717–4723
- Uddin MJ, Cesano F, Bonino F, Bordiga S, Spoto G, Scarano D, Zecchina A (2007) Photoactive TiO₂ films on cellulose fibres: synthesis and characterization. *J Photoch Photobio A* 189:286–294. <https://doi.org/10.1016/j.jphotochem.2007.02.015>
- Ugur SS, Sarusik M, Aktas H (2010) The fabrication of nanocomposite thin films with TiO₂ nanoparticles by the layer-by-layer deposition method for multifunctional cotton fabrics. *Nanotechnology* 21:325603. <https://doi.org/10.1088/0957-4484/21/32/325603>
- Wu Y, Hong-Mei L, Bo-Qing X, Zao-Li Z, Dang-Sheng S (2007) Single-phase titania nanocrystallites and nanofibers from titanium tetrachloride in acetone and other ketones. *Inorg Chem* 46:5093–5099. <https://doi.org/10.1021/ic070199h>
- Yaqoob AA, Umar K, Ibrahim MNM (2020) Silver nanoparticles: various methods of synthesis, size affecting factors and their potential applications—a review. *Appl Nanosci* 10:1369–1378. <https://doi.org/10.1007/s13204-020-01318-w>
- Yocupicio-Gaxiola RI, Petranovskii V, Sánchez P, Antúnez-García J, Alonso-Núñez G, Galván DH, Murrieta-Rico FN (2021) Prospects for further development of face masks to minimize pandemics – functionalization of textile materials with biocide inorganic nanoparticles: a review. *IEEE Lat Am Trans* 19:1010–1023. <https://doi.org/10.1109/TLA.2021.9451247>

Publisher's Note Springer Nature remains neutral with regard to jurisdictional claims in published maps and institutional affiliations.

Springer Nature or its licensor holds exclusive rights to this article under a publishing agreement with the author(s) or other rightsholder(s); author self-archiving of the accepted manuscript version of this article is solely governed by the terms of such publishing agreement and applicable law.